JAPANESE DERMATOLOGICAL ASSOCIATION
THE JOURNAL OF DERMATOLOGY

doi: 10.1111/j.1346-8138.2010.00932.x

Journal of Dermatology 2010; **37**: 956–964

ORIGINAL ARTICLE

Expression of wild-type, but not mutant, loricrin causes programmed cell death in HaCaT keratinocytes

Kozo YONEDA,[1] Toshio DEMITSU,[2] Motomu MANABE,[3] Junsuke IGARASHI,[4] Hiroaki KOSAKA,[4] Nobuya INAGAKI,[5] Hidetoshi TAKAHASHI,[6] Atsushi KON,[7] Maki KAKURAI,[2] Yasuo KUBOTA[1]

[1]Department of Dermatology, Faculty of Medicine, Kagawa University, Kagawa, [2]Department of Dermatology, Jichi Medical University Omiya Medical Center, Saitama, [3]Department of Dermatology, Akita University School of Medicine, Akita, [4]Cardiovascular Physiology, Faculty of Medicine, Kagawa University, Kagawa, [5]Department of Diabetes and Clinical Nutrition, Kyoto University Graduate School of Medicine, Kyoto, [6]Department of Dermatology, Asahikawa Medical College, Hokkaido, and [7]Department of Biochemistry, Hirosaki University School of Medicine, Hirosaki, Japan

ABSTRACT

The epidermal cornified cell envelope is a complex protein–lipid composite that replaces the plasma membrane of corneocytes and is crucial for epidermal barrier function. Loricrin is a major constituent of the epidermal cornified cell envelope, contributing approximately 70% by mass. In order to explore novel function of wild-type (WT) loricrin other than the major component of the epidermal cornified cell envelope, we transiently expressed construct encoding human WT and mutant loricrin (730insG) in HaCaT keratinocytes. HaCaT cells transfected with WT or mutant loricrin were at differentiation level. WT loricrin in the transfected cells was seen diffusely in the cytoplasm and nuclei. Positive transferase deoxytidyl uridine end labeling staining was observed in the nuclei of WT loricrin-transfected HaCaT keratinocytes. Data from the DNA fragmentation assay showed that only WT loricrin induced DNA ladders compared with that of mutant loricrin. WT loricrin-transfected HaCaT keratinocytes were susceptible to programmed cell death (PCD). Activation of caspase-14 was also seen. In contrast, PCD or activation of caspase-14 did not occur in mutant loricrin-transfected HaCaT cells. These results suggest that the expression of WT loricrin facilitates induction of PCD in HaCaT keratinocytes.

Key words: caspase-14, cornified cell envelope, loricrin, programmed cell death.

INTRODUCTION

Loricrin is a glycine-, serine- and cystein-rich basic protein expressed in the granular cell layer of the epidermis, where it is first stored in aggregates (L-granules in mouse, keratohyalin granules in human) that are predominantly cytoplasmic, but also seen in the nucleus.[1–6] In the last stage of terminal differentiation, these aggregates are dispersed and loricrin is assembled into the cornified cell envelope where it is cross-linked with the other cornified cell envelope components. Recently, mutations in the loricrin gene have been reported in Vohwinkel syndrome with ichthyosis (Online Mendelian Inheritance in Man [OMIM] 604117).[7–17] Furthermore, Ishida-Yamamoto *et al.*[14] identified a similar loricrin mutation in a family with progressive symmetric erythrokeratoderma (OMIM 602036). These syndromes are now collectively named loricrin keratoderma. So far, four types of loricrin mutations have been detected in genomic DNA from nine families. The most frequent mutation, 730insG, has been found in families from the UK, Japan and Germany. A defective protein generated from the mutant loricrin allele in Vohwinkel syndrome

Correspondence: Kozo Yoneda, M.D., Ph.D., Department of Dermatology, Faculty of Medicine, Kagawa University, Kagawa 761-0793, Japan.
Email: kyoneda@med.kagawa-u.ac.jp
Received 9 February 2010; accepted 28 March 2010.

is unusual. It generates a frame-shift before its terminal 84 codons, which further extends the polypeptide 22 amino acids beyond the C-terminal domain of the wild-type (WT) protein. This C-terminal domain of the mutant, but not WT, loricrin polypeptide is predicted to contain a nuclear localization signal. To explore the molecular mechanisms for abnormal keratinization caused by mutant loricrin, it is essential to know the function of WT and mutant loricrin *in vivo* and *in vitro*.

In this study, we sought to determine the function of WT loricrin in HaCaT keratinocytes using transient transfection as a means of ectopic protein expression. We report here that expression of human WT, but not mutant, loricrin leads to programmed cell death (PCD) with the activation of caspase-14.

METHODS

Plasmid construction

Genomic DNA containing the entire coding region of WT loricrin[1] and mutant loricrin[10] was subcloned into pcDNA 3.1/V5-His vector (Invitrogen, San Diego, CA, USA). The most frequent mutation, 730insG, was chosen for the present study. The sequence of each of the plasmid constructs was verified by the dideoxynucleotide chain termination method using the 377 DNA sequencing system (Applied Biosystems, Foster City, CA, USA).

Cell culture and plasmid transfection

The culture and transfection of HaCaT cells were carried out as previously described.[18,19] Briefly, cells were plated on 35 or 60 mm culture dishes at a density of 4×10^5 cells/mL 24 h before plasmid transfection, and cultured in Dulbecco's modified Eagle's medium (450 mg/dL glucose) supplemented with 10% (v/v) fetal bovine serum. A portion of 2 μg of WT loricrin or mutant loricrin in pcDNA3.1/V5-His vector for 35-mm dishes and 10 μg for 100-mm dishes was transfected into cells with LipofectAMINE plus reagent (Invitrogen) according to the manufacturer's instructions. Forty-eight hours after transfection, cells were collected for further analysis. In each experiment, transfection efficiency was confirmed to be similar among types of transfected plasmids using X-gal staining. The percentage of cell death induced by WT loricrin was determined by transfecting cells with pcDNA3.1/V5-His vector (mock), pcDNA3.1/V5-His WT loricrin and pcDNA3.1/V5-His mutant loricrin. PCD cells were identified by visual inspection with a Nikon inverted fluorescence microscope (Nikon, Tokyo, Japan). The uptake of Trypan blue and SYTO 13 (Invitrogen) was used to confirm the number of PCD. Each experiment was performed at least five times, with 10 000 cells counted for each determination.

Primary antibodies

The anti-V5 antibody was purchased from Invitrogen, polyclonal rabbit anti-human keratin antibody from DAKO (Glostrup, Denmark), anti-caspase-14, anti-filaggrin, anti-transglutaminase-1, anti-involucrin and anti-α-tubulin antibody from Santa Cruz Biotech (Santa Cruz, CA, USA), and anti-envoplakin and anti-periplakin antibody from Abcam (Cambridge, UK).

Immunofluorescence microscopy

Immunostaining was performed exactly as described previously.[20] After 48 h of transfection, HaCaT cells on glass coverslips were fixed with methanol. Cells on glass coverslips were incubated with primary antibodies (anti-V5 [1:300], anti-keratin [1:200], anti-envoplakin [1:300], anti-periplakin [1:300], anti-involucrin [1:300], anti-transglutaminase-1 [1:300], and anti-filaggrin [1:300]) overnight at 4°C, and detection was made with fluorescein isothiocyanate-conjugated antibody to rabbit immunoglobulin (Ig)G or a combination of Cy3-conjugated streptavidin and biotin-conjugated antimouse IgG. Immunofluorescent images were viewed with a confocal laser microscope (Olympus, Tokyo, Japan).

Immunoblot analysis

Immunoblot analysis was performed exactly as described previously.[18] After 48 h of transfection, HaCaT cells were lysed in Laemli buffer (consisting of 62.5 mmol/L Tris-HCl (pH 6.8), 25% glycerol, 2% sodium dodecylsulfate [SDS], 0.01% bromphenol blue) on ice for 30 min. Cell debris was removed by centrifugation at 20 380 *g* for 1 min, and supernatant (cell lysates) was collected. Protein concentrations in cell lysates were determined using Bradford reagent (BioRad, Hercules, CA, USA). Cell lysates containing 30 μg proteins were electrophoresed on an SDS/polyacrylamide gel and transferred to a nitrocellulose membrane. The membrane was incubated with

primary antibody (anti-V5 [1:1000], anti-caspase-14 [1:5000] and anti-α-tubulin [1:200] antibody) for 2 h at room temperature, followed by incubation with horseradish peroxidase (HRP)-conjugated appropriate secondary antibody, and the proteins were detected using an enhanced chemiluminescence system (Amersham Biosciences, Piscataway, NJ, USA) according to the manufacturer's instructions.

TUNEL staining

Transferase deoxytidyl uridine end labeling (TUNEL) staining was performed with ApopTag apoptosis detection kit (Intergen, Burlington, MA, USA) exactly as described previously.[18] HaCaT cells on coverslips were fixed with −20°C methanol, rinsed with phosphate buffered saline (PBS) two times, and treated with 10% normal goat serum for 10 min. They were then incubated with the anti-V5 antibody for 30 min, rinsed with PBS three times, and incubated with biotin-conjugated goat antimouse IgG (Sigma, St Louis, MO, USA) for 30 min, followed by incubation with streptavidin–Cy3 conjugate (Sigma) for 30 min. Cells were incubated with working strength TdT enzyme at 37°C for 1 h, extensively washed with stop/wash buffer and PBS, and incubated with anti-digoxigenin conjugate fluorescent dye for 30 min. They were mounted on a glass slide with PermaFluor (Thermo-Shandon, Vernon Hills, IL, USA) and observed by confocal laser microscope (Olympus).

DNA fragmentation assay

After 48 h of transfection, HaCaT cells were lysed in lysis buffer (10 mmol/L Tris-HCl (pH 8.0), 100 mmol/L NaCl, 1% SDS, 1 mmol/L ethylene diamine tetra acetate, and 2 mg/mL proteinase K) for 1 h at 65°C. Following two successive extractions with phenol/chloroform, the DNA samples were precipitated in ethanol. After washing with 70% ethanol, the DNA samples were resuspended in TE buffer and subjected to 2% agarose gel electrophoresis.

Statistics

All values are presented as means ± standard error of the mean. The significance of the difference from the respective controls for each experiment test condition was assayed using a Student's *t*-test for each paired experiment. An ANOVA was used to test for significance ($P < 0.05$).

RESULTS

Subcellular localization of WT and mutant loricrin

Genomic DNA containing the coding region of WT loricrin and mutant loricrin was subcloned into pcDNA3.1/V5-His vector. The most frequent mutation, 730insG, was chosen for this study. The transfection efficiencies for WT and mutant loricrin were almost the same. Immunoblot analysis using anti-V5 antibody revealed that WT loricrin (Fig. 1a, arrow, 35 kDa) and mutant loricrin (arrowhead, 42 kDa) were expressed to almost the same degree (Fig. 1a). Although the expected molecular mass of WT loricrin is 35 kDa, the migrating position of WT loricrin was around the 37-kDa molecular marker. We think this migration is due to many aliphatic amino acids (glycine/serine/cystein) in WT loricrin. Next, to determine whether mutant loricrin protein localizes in the nucleus in cultured keratinocytes as in keratinocytes of loricrin keratoderma *in vivo*,[7] we transfected HaCaT cells with V5-tagged WT loricrin or mutant loricrin, the mutation in loricrin keratoderma, and stained them with an anti-V5 antibody and an anti-keratin antibody. WT loricrin distributes in the cytoplasm and nucleus (Fig. 1b, upper right panel). Mutant loricrin, which is predicted to get a nuclear localization signal, seems to localize in the nucleolus (Fig. 1c, upper right panel). Why it localizes in the nucleolus, rather than nucleus, is not clear as reported by Ishida-Yamamoto *et al.*[21] We analyzed 4 000 000 cells and found that transfection efficiency was the same in either semi-confluent or non-confluent state. That is, transfection efficiency was not dependent on confluency. When WT loricrin was transfected, we observed cells shrinking perhaps due to PCD.

Differentiation level of the HaCaT cells transfected with WT or mutant loricrin

At first, we transfected WT loricrin and mutant loricrin into normal human epidermal keratinocytes. Normal human epidermal keratinocytes were purchased from KURABO (Osaka, Japan). These primary human epidermal keratinocytes were cultured and transfected as described by DiColandrea *et al.*[22] However, we could not transfect WT and mutant loricrin constructs into normal human epidermal keratinocytes. That was

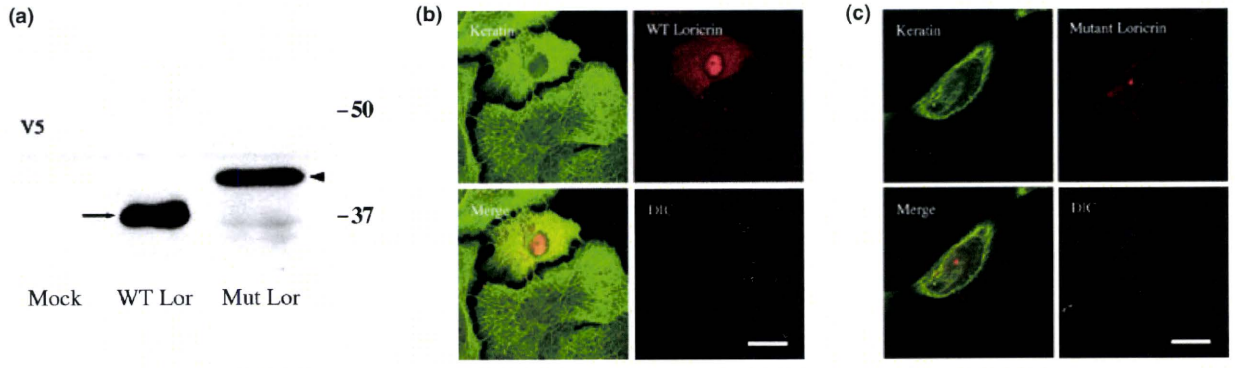

Figure 1. (a) Immunoblot analysis of wild-type (WT) loricrin-transfected HaCaT cells and mutant loricrn-transfected HaCaT cells. Immunoblot with anti-V5 antibody revealed that WT loricrin and mutant loricrin were expressed to almost the same degree. Arrow denotes 35-kDa WT loricrin including V5 tag sequence. Arrowhead denotes 42-kDa mutant loricrin including V5 tag sequence. Although the expected molecular mass of WT loricrin is 35 kDa, the migrating position of WT loricrin was around the 37-kDa molecular marker. We think this migration is due to many aliphatic amino acids (glycine/serine/cystein) in WT loricrin. (b,c) Distribution of WT loricrin-V5 and mutant loricrin-V5 of transfected HaCaT keratinocytes. HaCaT keratinocytes were transfected with either plasmid pcDNA3.1/V5-His-WT loricrin or plasmid pcDNA3.1/V5-His-mutant loricrin. Cells were fixed at 48 h post-transfection, and the fate of the transfected gene product was examined by double-label immunofluorescence. To visualize the transfected gene product, cells were stained with a mouse monoclonal antibody recognizing the sequence of V5. Antibody staining was followed by biotin-conjugated antimouse immunoglobulin G and Cy3-conjugated streptavidin. (b) Double-stainings of HaCaT cells with 1:100-diluted anti-V5 antibody (red) and 1:100-diluted anti-keratin antibody (green). WT loricrin distributes diffusely in the cytoplasm and in the nuclei in transfected cells. (Scale bars: 25 μm.) (c) Double-stainings of HaCaT cells with 1:100-diluted anti-V5 antibody (red) and 1:100-diluted anti-keratin antibody (green). Mutant loricrin distributes in the nucleolus as a V5-positive immunoreactive granule. (Scale bars: 25 μm.) DIC, differential interference contrast.

to say, transfection efficiency was so low (<0.1%) that we could not detect WT or mutant loricrin with immunoblot analysis. Then, we decided to use HaCaT cells. The HaCaT keratinocyte cell line is a spontaneously transformed human epithelial cell line derived from adult skin which maintains full epidermal differentiation capacity.[23] The transfection efficiency into HaCaT cells was approximately 3%. Because the expression of WT and mutant loricrin is observed only in morphologically different keratinocytes, we tried to estimate the differentiation level of WT and mutant loricrin transfected HaCaT cells. WT loricrin-transfected HaCaT cells exhibited positive immunoreactivities for periplakin, envoplakin, involucrin, transglutaminase 1 and filaggrin. Mutant loricrin-transfected HaCaT cells also exhibited positive immunoreactivities for periplakin, envoplakin, involucrin, transglutaminase 1 and filaggrin. Mutant loricrin in the nucleoli co-localized with periplakin, envoplakin, involucrin, transglutaminase 1 and filaggrin (Fig. 2). We could not transfect WT or mutant loricrin into non-differentiated level HaCaT cells (filaggrin-negative HaCaT cells). These results suggest that HaCaT cells expressing WT or mutant loricrin are at differentiation level because periplakin, envoplakin, involucrin, transglutaminase 1 and filaggrin are differentiation markers.

PCD and activation of caspases-14 in HaCaT cells expressing WT loricrin

To explore whether WT loricrin induces PCD in HaCaT cells, we first examined the effects of WT loricrin on cell morphology. Forty-eight hours after transfection, the number of cell deaths was determined by counting 10 000 HaCaT cells under a phase-contrast microsocpe. PCD cells were judged by staining both PCD nuclei with SYTO 13 and plasma-membrane permeabilization with Trypan blue. When WT loricrin was transfected, PCD cells which contained PCD nuclei were increased (Fig. 3a). PCD cells in 10 000 cells increased from 9 ± 2.2 of mock to 103 ± 4.3 of WT loricrin. In contrast, mutant loricrin did not increase PCD cells (8 ± 4.1 cells).

Furthermore, positive TUNEL stainings were observed in the nuclei in WT loricrin-transfected cells (Fig. 3b). Data from the DNA fragmentation assay showed that only WT loricrin induced DNA ladders

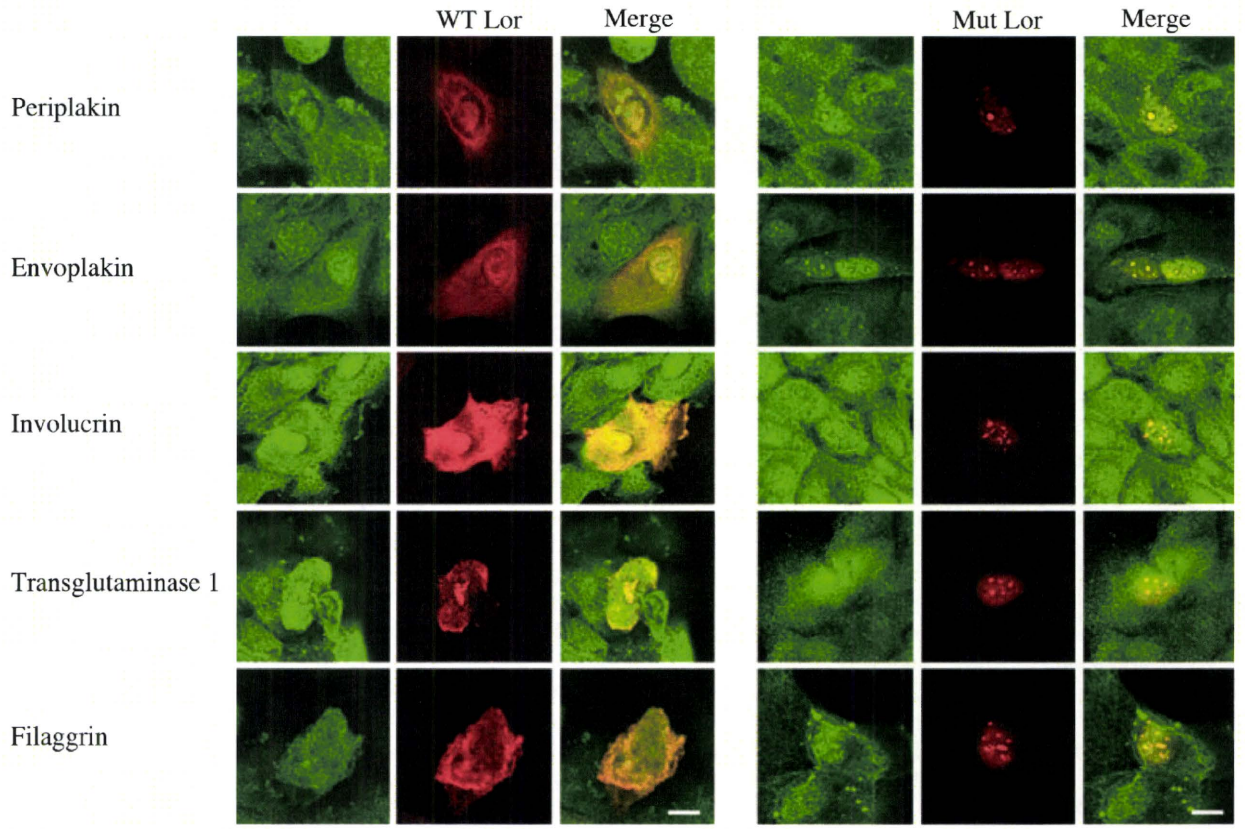

Figure 2. Differentiation level of the HaCaT cells after transfection of wild-type (WT) and mutant loricrin. WT loricrin-transfected HaCaT cells exhibited positive immunoreactivities for periplakin, envoplakin, involucrin, transglutaminase 1 and filaggrin. Mutant loricrin-transfected HaCaT cell also exhibited positive immunoreactivities for periplakin, envoplakin, involucrin, transglutaminase 1 and filaggrin. We could not transfect WT or mutant loricrin into non-differentiated level HaCaT cells (filaggrin-negative HaCaT cells). (Scale bars: 25 μm.)

(Fig. 3c). Immunoblot analysis using anti-caspase-14 antibody revealed that processing the p11 fragment was observed only in WT loricrin-transfected cells (Fig. 3d, arrow). Caspase-14 was not activated in mock or mutant loricrin-transfected HaCaT cells.

DISCUSSION

As far as we know, we showed for the first time that procaspase-14 was processed and activated accompanying PCD when we transfected WT loricrin in HaCaT cells. In contrast, transient expression of mutant loricrin in HaCaT keratinocytes does not result in PCD or activation of casapse-14. The number of PCD cells in cells transfected with WT loricrin was markedly higher than that in cells of transfected mock or mutant loricrin. In addition, we showed positive TUNEL staining in WT loricrin-transfected cells. Although we demonstrated that PCD occurred in the HaCaT cells after transient transfection of WT loricrin, we assume that this response represents a tissue-specific form of PCD that differs from classical apoptosis. The frame-shift mutations in the loricrin gene have produced mutant forms of loricrin with altered and extended COOH termini, as a consequence of alternative, downstream termination signals. Thus, the common feature of all loricrin mutations described to date is replacement of the COOH-terminal Gly- and Gln/Lys-rich domain with highly charged Arg- and Leu-rich domain amino acid sequences. Because the COOH-terminus of mutant loricrin is very different from the WT loricrin, namely, acquiring a nuclear localization signal, mutant loricrin accumulates in the nucleus. Mutant loricrin overexpressed in HaCaT cells by transfection did not cause PCD *in vitro*, which might be related to pathogenesis of

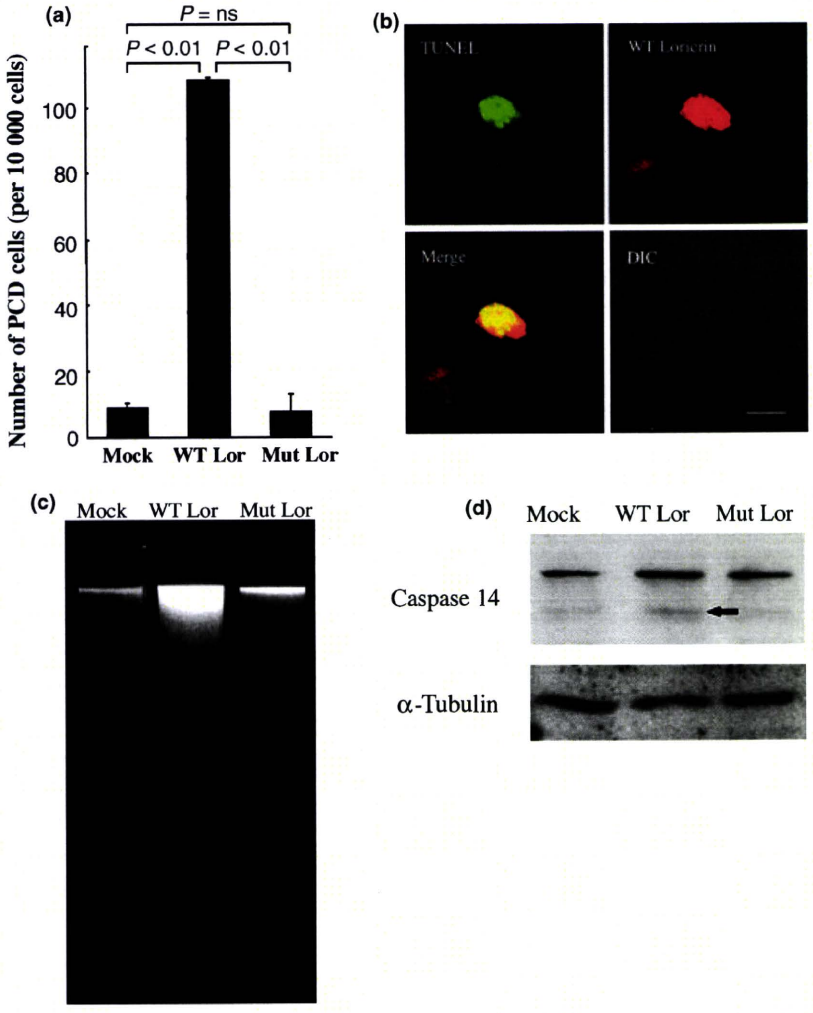

Figure 3. Induction of programmed cell death (PCD) by wild-type (WT) loricrin but not by mutant loricrin. (a) Number of PCD cells was significantly higher in WT loricrin than in mock or mutant loricrin (morphology) (n = 5). Quantification of PCD was performed by both staining PCD nuclei with SYTO 13 and plasma-membrane permeabilization with Trypan blue. (b) Double-stainings with 1:100-diluted anti-V5 antibody (red; upper right panel) and transferase deoxytidyl uridine end labeling (TUNEL) staining (green; upper left panel). Lower left panel shows merge of the two stainings. Positive TUNEL stainings were observed in the nuclei in WT loricrin-transfected cells. (Scale bars: 25 μm.) (c) Data from the DNA fragmentation assay showed that only WT loricrin induced DNA ladders. (d) Activation of caspase-14 by WT loricrin. Immunoblot with 1:5000 diluted anti-caspase-14 and with 1:200 diluted anti-α-tubulin antibody. Caspase-14 was activated in WT loricrin-transfected cells. Similar data were obtained in five experiments. DIC, differential interference contrast.

keratoderma although more studies are needed. Ishida-Yamamoto *et al.*[16] reported that number of TUNEL-positive cells was increased in the skin of loricrin keratoderma. They reported that epidermal differentiation in loricrin keratoderma seemed to be disrupted at the very late stages, immediately before the disintegration of apoptotic nuclei containing profilaggrin amino-terminus. Anti-apoptotic protein, such as Mcl-1, might be expressed more abundantly in HaCaT cells than *in vivo* epidermis because HaCaT cells were spontaneously immortalized an aneuploid human keratinocyte cell line.[24]

Filaggrin is an intermediate filament-associated protein that aggregates epidermal keratin filaments *in vitro* and is thought to perform a similar function during terminal differentiation *in vivo*. Loricrin and filaggrin are two major proteins expressed by terminally differentiated epidermal keratinocytes. Recently,

the importance of filaggrin has been underscored by demonstrating that loss-of-function mutations in the profilaggrin gene underlie the skin disease ichthyosis vulgaris, and that they strongly predispose to atopic dermatitis and asthma.[25,26] Dale *et al.*[27] showed that transient expression of filaggrin in epithelial cells led cell contraction, nuclear membrane breakdown and nuclear condensation. Dale *et al.*[27] and Kuechle *et al.*[28] stated that a low transfection rate is also seen in filaggrin constructs (<2%) as we observed with WT and mutant loricrin constructs. They reported that green fluorescent protein (GFP) and β-galactosidase control constructs showed 15–20% transfection rate. We also observed that the transfection rate of pcDNA3.1/V5-His WT keratin 14 was 20–30%. We also tried Lipofectamine 2000 (Invitrogen) as a transfection reagent. However, transfection efficiency of loricrin was almost the same as using LipofectAMINE plus reagent (Invitrogen). The reason why there is disparity in transfection rate between loricrin and keratin 14 constructs is not currently clear. In addition, we could not detect proteins by immunoblot analysis after transfection of WT and mutant loricrin constructs into cultured normal human epidermal keratinocytes. Similarly, we observed a cystatin A expression vector with cytomegalovirus immediate early promoter could not transfect cystatin A in cultured normal human epidermal keratinocytes.[29] Transfection of cornified cell envelope component proteins such as loricrin, filaggrin or cystatin A into cultured keratinocytes may be very difficult.

We formerly showed that no alterations could be observed in mice with an approximately twofold overexpression of human WT loricrin.[3] We also observed that human cystatin A transgenic mice did not show any abnormalities in the epidermis or hair follicle.[29] Presland *et al.*[30] created human filaggrin transgenic mice and observed no abnormalities in the epidermis, hair structures or tissue organization. Interestingly enough, there was no evidence of altered keratin filament organization in the suprabasal layers of filaggrin transgenic epidermis. On the contrary to these transgenic mice *in vivo* data, we observed that WT loricrin-transfected HaCaT keratinocytes were susceptible to PCD. Dale *et al.*[27] proved that transient transfection of epidermal filaggrin efficiently aggregates keratin filaments when expressed *in vitro* either in rat keratinocytes (keratin5/keratin14 and keratin1/keratin10) or monkey COS-7 cells (keratin8/keratin18). Presland *et al.*[30,31] reported that there was a disruption of cell–cell adhesion in keratinocytes overexpressing filaggrin, which they did not observe in transgenic mice overexpressing filaggrin. They speculated that cultured cells might be more sensitive to keratin filament disruption than epidermal tissue, which expressed a greater diversity of keratin proteins and thus contained a more robust intermediate filament network with stronger cell–cell adhesion through desmosomes. Similarly, we think cultured HaCaT cells may be more sensitive to various PCD stimuli than *in vivo* epidermal tissue which express a greater diversity of keratin proteins and contain an abundant type I keratin proteins that are known to prevent apoptosis.

Although the bulk of WT loricrin exists within keratohyalin granules and cornified cell envelope, WT loricrin is also known to be present in the nucleus at *in vivo* epidermis.[4] We also confirm that WT loricrin distributes in the nucleus *in vitro* transfected HaCaT cells. However, the function of WT loricrin is not known yet. The profilaggrin N-terminal domain localizes to both cytoplasm and nucleus of epidermal granular layer cells. Profilaggrin is a large phosphoprotein that is expressed in the granular cells of epidermis where it is localized in keratohyalin. It consists of multiple copies of single filaggrin units plus N- and C-terminal sequences that differ from filaggrin. The N-terminal sequence of human profilaggrin comprises two distinct domains; an acidic A domain of 81 amino acids that binds calcium, and a cationic B domain of 212 residues. The cellular distribution of WT loricrin is similar to that of profilaggrin N-terminal domain. We speculate that WT loricrin may interact with profilaggrin N-terminal domain *in vivo* and that this interaction may have some role in normal epidermal keratinization. To explore the expression of nuclear WT loricrin in cultured keratinocytes and epidermis and examine its association with profilaggrin N-terminal domain would be of great interest as a future project.

In summary, this study shows that expression of WT loricrin in HaCaT keratinocytes causes PCD whereas mutant loricrin is unable to cause PCD. Our results may implicate novel function of WT loricrin considering that the overexpression of filaggrin and profilaggrin results in PCD in both simple epithelial cells (COS-7) and rat epidermal keratinocyte cell line (REK).[27]

ACKNOWLEDGMENTS

We are grateful to Dr N. Fusenig for HaCaT cells; F. Naruse, T. Takamura and F. Nishiyama for technical assistance and artwork. This work was in part supported by grants from the Ministries of Health, Labor and Welfare and Education, Culture, Sports, Science, and Technology of Japan.

REFERENCES

1 Yoneda K, Hohl D, McBride OW *et al.* The human loricrin gene. *J Biol Chem* 1992; **267**: 18060–18066.
2 Yoneda K, McBride OW, Korge BP, Kim IG, Steinert PM. The cornified cell envelope: loricrin and transglutaminases. *J Dermatol* 1992; **19**: 761–764.
3 Yoneda K, Steinert PM. Overexpression of human loricrin in transgenic mice produces a normal phenotype. *Proc Natl Acad Sci USA* 1993; **90**: 10754–10758.
4 Ishida-Yamamoto A, Hohl D, Roop DR, Iizuka H, Eady RA. Loricrin immunoreactivity in human skin: localization to specific granules (L-granules) in acrosyringia. *Arch Dermatol Res* 1993; **285**: 491–498.
5 Ishida-Yamamoto A. Loricrin keratoderma: a novel disease entity characterized by nuclear accumulation of mutant loricrin. *J Dermatol Sci* 2003; **31**: 3–8.
6 Bickenbach JR, Greer JM, Bundman DS, Rothnagel JA, Roop DR. Loricrin expression is coordinated with other epidermal proteins and the appearance of lipid lamellar granules in development. *J Invest Dermatol* 1995; **104**: 405–410.
7 Maestrini E, Monaco AP, McGrath JA *et al.* A molecular defect in loricrin, the major component of the cornified cell envelope, underlies Vohwinkel's syndrome. *Nat Genet* 1996; **13**: 70–77.
8 Korge BP, Ishida-Yamamoto A, Punter C *et al.* Loricrin mutation in Vohwinkel's keratoderma is unique to the variant with ichthyosis. *J Invest Dermatol* 1997; **109**: 604–610.
9 Armstrong DK, McKenna KE, Hughes AE. A novel insertional mutation in loricrin in Vohwinkel's Keratoderma. *J Invest Dermatol* 1998; **111**: 702–704.
10 Takahashi H, Ishida-Yamamoto A, Kishi A, Ohara K, Iizuka H. Loricrin gene mutation in a Japanese patient of Vohwinkel's syndrome. *J Dermatol Sci* 1999; **19**: 44–47.
11 Matsumoto K, Muto M, Seki S *et al.* Loricrin keratoderma: a cause of congenital ichthyosiform erythroderma and collodion baby. *Br J Dermatol* 2001; **145**: 657–660.
12 O'Driscoll J, Muston GC, McGrath JA, Lam HM, Ashworth J, Christiano AM. A recurrent mutation in the loricrin gene underlies the ichthyotic variant of Vohwinkel syndrome. *Clin Exp Dermatol* 2002; **27**: 243–246.
13 Gedicke MM, Traupe H, Fischer B, Tinschert S, Hennies HC. Towards characterization of palmoplantar keratoderma caused by gain-of-function mutation in loricrin: analysis of a family and review of the literature. *Br J Dermatol* 2006; **154**: 167–171.
14 Ishida-Yamamoto A, McGrath JA, Lam H, Iizuka H, Friedman RA, Christiano AM. The molecular pathology of progressive symmetric erythrokeratoderma: a frameshift mutation in the loricrin gene and perturbations in the cornified cell envelope. *Am J Hum Genet* 1997; **61**: 581–589.
15 Ishida-Yamamoto A, Takahashi H, Iizuka H. Loricrin and human skin diseases: molecular basis of loricrin keratodermas. *Histol Histopathol* 1998; **13**: 819–826.
16 Ishida-Yamamoto A, Takahashi H, Presland RB, Dale BA, Iizuka H. Translocation of profilaggrin N-terminal domain into keratinocyte nuclei with fragmented DNA in normal human skin and loricrin keratoderma. *Lab Invest* 1998; **78**: 1245–1253.
17 Song S, Shen C, Song G *et al.* A novel c.545-546insG mutation in the loricrin gene correlates with a heterogeneous phenotype of loricrin keratoderma. *Br J Dermatol* 2008; **159**: 714–719.
18 Yoneda K, Furukawa T, Zheng YJ *et al.* An autocrine/paracrine loop linking keratin 14 aggregates to tumor necrosis factor alpha-mediated cytotoxicity in a keratinocyte model of epidermolysis bullosa simplex. *J Biol Chem* 2004; **279**: 7296–7303.
19 Inoue T, Yoneda K, Manabe M, Demitsu T. Spontaneous regression of merkel cell carcinoma: a comparative study of TUNEL index and tumor-infiltrating lymphocytes between spontaneous regression and non-regression group. *J Dermatol Sci* 2000; **24**: 203–211.
20 Yoneda K, Fujimoto T, Imamura S, Ogawa K. Distribution of fodrin in the keratinocyte *in vivo* and *in vitro*. *J Invest Dermatol* 1990; **94**: 724–729.
21 Ishida-Yamamoto A, Kato H, Kiyama H *et al.* Mutant loricrin is not crosslinked into the cornified cell envelope but is translocated into the nucleus in loricrin keratoderma. *J Invest Dermatol* 2000; **115**: 1088–1094.
22 DiColandrea T, Karashima T, Maatta A, Watt FM. Subcellular distribution of envoplakin and periplakin: insights into their role as precursors of the epidermal cornified envelope. *J Cell Biol* 2000; **151**: 573–586.
23 Boukamp P, Petrussevska RT, Breitkreutz D, Hornung J, Markham A, Fusenig NE. Normal keratinization in a spontaneously immortalized aneuploid human keratinocyte cell line. *J Cell Biol* 1988; **106**: 761–771.
24 Sitailo LA, Jerome-Morais A, Denning MF. Mcl-1 functions as major epidermal survival protein required for proper kertinocyte differentiation. *J Invest Dermatol* 2009; **129**: 1351–1360.

25 Smith FJ, Irvine AD, Terron-Kwiatkowski A *et al.* Loss-of-function mutations in the gene encoding filaggrin cause ichthyosis vulgaris. *Nat Genet* 2006; **38**: 337–342.
26 Palmer CN, Irvine AD, Terron-Kwiatkowski A *et al.* Common loss-of-function variants of the epidermal barrier protein filaggrin are a major predisposing factor for atopic dermatitis. *Nat Genet* 2006; **38**: 441–446.
27 Dale BA, Presland RB, Lewis SP, Underwood RA, Fleckman P. Transient expression of epidermal filaggrin in cultured cells causes collapse of intermediate filament networks with alteration of cell shape and nuclear integrity. *J Invest Dermatol* 1997; **108**: 179–187.
28 Kuechle MK, Presland RB, Lewis SP, Fleckman P, Dale BA. Inducible expression of filaggrin increases keratinocyte susceptibility to apoptotic cell death. *Cell Death Differ* 2000; **7**: 566–573.
29 Takahashi H, Komatsu N, Ibe M, Ishida-Yamamoto A, Hashimoto Y, Iizuka H. Cystatin A suppresses ultraviolet B-induced apoptosis of keratinocytes. *J Dermatol Sci* 2007; **46**: 179–187.
30 Presland RB, Coulombe PA, Eckert RL, Mao-Qiang M, Feingold KR, Elias PM. Barrier function in transgenic mice overexpressing K16, involucrin, and filaggrin in the suprabasal epidermis. *J Invest Dermatol* 2004; **123**: 603–606.
31 Presland RB, Kuechle MK, Lewis SP, Fleckman P, Dale BA. Regulated expression of human filaggrin in keratinocytes results in cytoskeletal disruption, loss of cell-cell adhesion, and cell cycle arrest. *Exp Cell Res* 2001; **270**: 199–213.

Endocrine Journal 2010, **57** (6), 509-516

ORIGINAL

Phenotypical variety of insulin resistance in a family with a novel mutation of the insulin receptor gene

Ikuko Takahashi[1], Yuichiro Yamada[2], Hiroko Kadowaki[3,4], Momoko Horikoshi[4], Takashi Kadowaki[4], Takuma Narita[2], Satoko Tsuchida[1], Atsuko Noguchi[1], Akio Koizumi[5] and Tsutomu Takahashi[1]

[1] *Department of Pediatrics, Akita University Graduate School of Medicine, Akita, Japan*
[2] *Department of Endocrinology, Diabetes and Geriatric Medicine, Akita University Graduate School of Medicine, Akita, Japan*
[3] *Department of Child Studies, Kasei-Gakuin University, Tokyo, Japan*
[4] *Department of Metabolic Diseases, Graduate School of Medicine, University of Tokyo, Tokyo, Japan*
[5] *Department of Health and Environmental Sciences, Graduate School of Medicine, Kyoto University, Kyoto, Japan*

Abstract. A novel mutation of insulin receptor gene (INSR gene) was identified in a three generation family with phenotypical variety. Proband was a 12-year-old Japanese girl with type A insulin resistance. She showed diabetes mellitus with severe acanthosis nigricans and hyperinsulinemia without obesity. Using direct sequencing, a heterozygous nonsense mutation causing premature termination at amino acid 331 in the α subunit of INSR gene (R331X) was identified. Her father, 40 years old, was not obese but showed impaired glucose tolerance. Her paternal grandmother, 66 years old, has been suffered from diabetes mellitus for 15 years. Interestingly, they had the same mutation. One case of leprechaunism bearing homozygous mutation at codon 331 was identified. These findings led to the hypothesis that R331X may contribute to the variation of DM in the general population in Japan. An extensive search was done in 272 participants in a group medical examination that included 92 healthy cases of normoglycemia and 180 cases already diagnosed type 2 DM or detected hyperglycemia. The search, however, failed to detect any R331X mutation in this local population. In addition, the proband showed low level C-peptide/insulin molar ratio, indicating that this ratio is considered to be a useful index for identifying patients with genetic insulin resistance. In conclusion, a nonsense mutation causing premature termination after amino acid 331 in the α subunit of the insulin receptor was identified in Japanese diabetes patients. Further investigations are called for to address the molecular mechanism.

Key words: Insulin receptor, Insulin resistance, Type 2 diabetes, Leprechaunism, C-peptide/insulin molar ratio

THE INTERACTION of insulin with its cell surface receptor is the first step in insulin action and the first identified target of insulin resistance. Mutations in the insulin receptor gene lead to the insulin resistance in several syndromic forms. The human insulin receptor is encoded by a single gene with 22 exons and is an assembly of a disulfide bond-linked tetramer composed of two α and two β subunits [1-5]. After binding of insulin to the extracellular α subunit, the tyrosine kinase of the membrane spanning β subunit is activated and the receptor is autophosphorylated [6]. Insulin receptor kinase regulates the action of insulin on metabolism and growth through signal transduction pathways and is therefore thought to be central to insulin action [7].

Some dozens of mutations in the human insulin receptor gene have already been identified to date [8-11]. Homozygous or compound-heterozygous mutations in the insulin receptor gene are found in patients with syndromes of severe insulin resistance [12]. More severe Donohue syndrome ("Leprechaunism" OMIM 246200) and the milder Rabson-Mendenhall syndrome (OMIM 262190) are characterized by intrauterine and postnatal growth retardation, facial dysmorphism, lack of subcutaneous fat and altered glucose homeostasis with hyperinsulinemia, acanthosis nigricans and reduced life expectancy [13-15]. Cells from most patients with Donohue syndrome show absent or

Received Nov. 25, 2009; Accepted Feb. 18, 2010 as K09E-339
Released online in J-STAGE as advance publication Mar. 25, 2010
Correspondence to: Ikuko Takahashi, M.D., Department of Pediatrics, Akita University Graduate School of Medicine, Hondo 1-1-1, Akita-shi, Akita, 010-8543, Japan.
E-mail takaiku@doc.med.akita-u.ac.jp

severely reduced insulin binding, whereas those with Rabson-Mendenhall retain some insulin binding capacity. Therefore, it has been proposed that severity of the phenotype is determined by the degree of insulin resistance and that residual insulin binding capacity correlates with survival. Heterozygous mutations in the insulin receptor gene have been demonstrated in type A insulin resistance with the triad of insulin resistance, acanthosis nigricans, and hyperandrogenism (OMIM147670) [16].

In this study, we identified a heterozygous mutation causing premature termination at amino acid 331 substituting a termination codon for arginine in the L2 domain in α subunit of the insulin receptor gene in a Japanese patient with diabetes mellitus and hyperinsulinemia. Interestingly, her family members shared the same mutation but showed different clinical course.

Materials and Methods

Subjects

The proband, a girl of 12 years old, was referred to our hospital because of glucosuria detected by school urinary screening. She presented with mild symptoms of polydipsia and polyuria. She was born to unrelated Japanese parents at 37 weeks of gestation (birth weight 2495 g, birth length 48 cm). At birth, she did not have the dysmorphic features characteristic of leprechaunism or Rabson-Mendenhall syndrome, including intrauterine growth retardation, fasting hypoglycemia. Sensorineural hearing loss in right side was diagnosed when she was infant, but did not deteriorate.

At presentation, she was not obese, but showed severe acanthosis nigricans with scratching scar of her neck. It also mildly existed at the axilla and elbow. Hirsutism was not observed. Body mass index (BMI) was 21.6 (height 148.6 cm, weight 47.7 kg). Blood pressure was 110/70 mmHg. Pubertal stage was B2 and PH1. Laboratory tests revealed the following; HbA1c, 9.2 %; FPG, 124 mg/dL; IRI, 65.7 μU/mL; C-peptide, 3.18 ng/mL; AST, 20 IU/L; ALT, 18 IU/L; total cholesterol, 194 mg/dL; HDL cholesterol, 43.7 mg/dL; testosterone, 0.33 ng/mL. Islet associated autoantibodies were absent. Urine testing showed no ketonuria but proteinuria (microalbumin 64.4mg/g cr) and glucosuria. Ocular complication and retinopathy was not detected. Abdominal CT revealed no fatty liver and area of visceral fat on umbilical level was 41.8 cm^2 (normal: 60>). Although she showed diabetes mellitus with severe insulin resistance, her data of body composition was not suggested risk for obesity or metabolic syndrome. Self monitored blood glucose levels were 120-140 mg/dL at premeal time and 170-200 mg/dL at postprandial time. Her father, 40 years old, was healthy and no obesity (BMI 21.8) from a clinical point of view at the time of investigation. Her paternal grandmother, 66 years old, has been suffered from diabetes mellitus. She was also not obese (BMI 21.6) and has been treated with sulfonylureas for 15-years. She already developed retinopathy and presented vitreous hemorrhage 10 years ago. Her younger brother, seven years of age, had mild mental retardation and supported by special education. He showed mild obesity but normal response to oral glucose tolerance test without hyperinsulinemia (FPG, 86 mg/dL; IRI, 8.6 μU/mL; C-peptide, 1.53 ng/mL).

Measurements

The standard 75 g oral glucose tolerance test (OGTT) was performed, after overnight fast. Levels of glucose, insulin and C-peptide were measured at 0, 30, 60, 90 and 120 min. Insulin was measured using an enzyme immunoassay (E test TOSOH II; TOSOH Corporation, Tokyo, Japan). Cross-reactivity with proinsulin was 2 %. C-peptide was measured using a chemiluminescent enzyme immunoassay (LUMIPULSE Presto C-peptide; FUJIREBIO Inc., Tokyo, Japan). Proinsulin was measured using a RIA2 antibody method (HUMAN PROINSULIN RIA KIT; Linco Research Inc., St. Charles, MO).

We calculated C-peptide/insulin molar ratio from each molecular weight and international unit of insulin i.e. 26 IU/mg. We estimated molecular weight of insulin at 5800 and C-peptide at 3600. Consequently, 1 μU/mL of insulin is 6.09 pmol/L and 1 ng/mL of C-peptide is 0.278 nmol/L.

Sequence analysis

Informed consent was obtained from her family. Genomic DNA was extracted from peripheral blood lymphocytes using a DNA isolation kit for mammalian blood. Exon 1-2 of the insulin gene and Exons 1-22 of the insulin receptor gene were individually amplified using primer sets as described [17, 18]. PCR products were purified for direct sequence analysis on an ABI gene analyzer 310 or 3100 system according to the manufacturer's instructions (Applied Biosystems).

Analysis for prevalence of R331X mutant in population

We tested the frequency of R331X in type 2 DM or by chance hyperglycemia in adult people, living in the Akita prefecture located in northern Japan. We studied 272 participants of a group medical examination, comprised 92 healthy cases checked normoglycemia and 180 cases already diagnosed type 2 DM or detected hyperglycemia. These included 47 cases with family history of DM and 14 cases diagnosed before third decade. All participants gave informed consent, and the Ethics Committee of Kyoto University School of Medicine approved the study.

Genotyping of R331X was assayed with PCR restriction fragment length polymorphism. PCR reactions were conducted in a reaction volume of 7.5 μL with 20 ng genomic DNA, 2× GC buffer, 200 μM dNTPs, 10 pmol of each primer and 1 unit of LA Taq polymerase (Takara, Tokyo, Japan). The PCR primers used were 5′-AGATGTCTGAAGGACCTTGGA-3′ as a forward primer and 5′-ACAGCTCAGAGGGACATGGA-3′ as a reverse primer. PCR was performed with 39 cycles of the following 94°C for 45 s, 54°C for 45 s and 74°C for 1 min in a thermocycler. Obtained PCR products showed a single fragment at 285 bp. Six μL of 285-bp product were then digested with 2 units of BspCNI restriction enzyme at 25 °C for 2 h. Digestion products were visualized on a 3 % agarose gel. Wild-type allele produced double band at 269 and 16 bp and mutant allele produced three bands at 165, 104 and 16 bp.

Results

An OGTT revealed a diabetic pattern with hyperinsulinemia (Table 1). The homeostasis model assessment of insulin resistance (HOMA-IR), an index of insulin resistance, was 20.1. The C-peptide/insulin molar ratio was extremely low. The fasting and 120 min levels were 2.21 and 1.57, respectively (normal level of fasting is 4.0<). An insulin tolerance test (0.1U/kg insulin i.v.) showed insulin resistance with only 37 % reduction in plasma glucose levels. Metformin was started from 250 mg/day and increased up to 500 mg/day. HbA1c levels improved to 5-6 % six months later. At that point in time, her fasting proinsulin level was 71.7 pmol/L when the IRI level was 49.1 μg/mL. Proinsulin/insulin molar ratio was 0.24 (normal 0.1-0.2). Her insulin levels were still high; however, the acanthosis nigricans had disappeared after she had regained diabetic control.

Table 1 C-peptide/insulin molar ratio in family members

Patient

OGTT (1) on admission

Time (min)	0	30	60	90	120
PG (mg/dL)	124	224	263	280	262
IRI (μU/mL)	65.7	114.8	191.5	279.1	290.1
CPR (ng/mL)	3.18	4.62	7.01	9.80	10.00
CPR/IRI molar ratio	2.21	1.84	1.67	1.60	1.57

OGTT (2) 2 weeks after admission

Time (min)	0	30	60	90	120
PG (mg/dL)	85	190	224	220	202
IRI (μU/mL)	52.7	136.9	187.4	239.2	313.6
CPR (ng/mL)	2.68	5.80	8.00	8.99	10.50
CPR/IRI molar ratio	2.32	1.93	1.95	1.72	1.53

Father

OGTT

Time (min)	0	30	60	90	120
PG (mg/dL)	88	169	256	214	172
IRI (μU/mL)	10.1	37.0	100.5	108.1	110.5
CPR (ng/mL)	1.24	3.14	6.96	8.05	8.22
CPR/IRI molar ratio	5.60	3.87	3.16	3.40	3.40

Grandmother

Fasting time	
PG (mg/dL)	146
IRI (μU/mL)	30.1
CPR (ng/mL)	2.51
CPR/IRI molar ratio	3.84

Her clinical course suggested two genetic diseases of glucose metabolism. One was the insulin gene mutation, as characterized by a low level C-peptide/insulin molar ratio, and sometimes presents as type 2 DM. The other was the insulin receptor gene mutation, which clinically demonstrated type A insulin resistance.

A sequencing analysis of the 22 exons as well as the intron-exon junctions identified a heterozygous mutation at nucleotide position 1072 substituting a termination codon for arginine 331, a conserved amino acid in the insulin-like growth factor I receptor and insulin receptor-related receptor, in the putative receptor L2 domain of the patient's insulin receptor (Fig. 1) [19]. No other mutations were found in any of the insulin receptor genes analyzed in this study.

Her father and grandmother also had the same

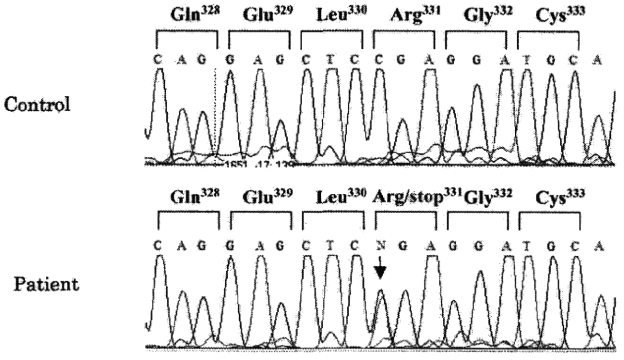

Fig. 1 Partial nucleotide sequence of the insulin receptor gene in the patient. Sequence from the patient is shown in comparison with that from the control. The patient is heterozygous for a mutation at the nucleotide position 1072, converting Arg 331(CGA) to a termination codon (TGA). An arrow indicates the position of mutation.

heterozygous mutation (data not shown). The fasting C-peptide/insulin molar ratio of her grandmother was relatively low under the treatment of sulfonylureas (3.84, IRI; 30.1 μU/mL, CPR 2.51 ng/mL). The HbA1c level of her father was 4.7 %, but OGTT showed impaired glucose tolerance (Table1). Although the fasting insulin level was 10.1 μU/mL, it increased up to 100 μU/mL in 60 -120 min. The C-peptide/insulin molar ratio was 5.60 in fasting and 3.40 in 120 min. They showed milder insulin resistance in comparison to the proband. The heterozygous mutation seemed to significantly affect the insulin resistance of the three subjects, even if no typical skin lesions were observed in either the father or grandmother.

One unrelated case of leprechaunism with R331X homozygous mutation was identified in Tokyo, Japan. The patient was born to unrelated parents at 39 weeks of gestation with a birth weight of 1743 g. She showed an extreme degree of insulin resistance (FPG, 200 mg/dL<; IRI 10,000 μU/mL<). She thereafter started to receive subcutaneous injections of recombinant human IGF-I. After treatment, her glucose metabolic abnormality was improved. Informed consent was obtained from her parents for sequence analysis. Her parents had R331X heterozygous mutation. They did not demonstrate any symptoms of diabetes mellitus. Information on the glucose tolerance including OGTT was unavailable.

These findings led to the hypothesis that insulin receptor genetic variants contribute to the variation of DM in the general population in Japan. An extensive search was done in 272 participants in a group medical examination that included 92 healthy cases of normoglycemia and 180 cases already diagnosed as type 2 DM or detected hyperglycemia. The search, however, failed to detect any R331X mutation in this local population.

Discussion

Type A insulin resistance was initially characterized in young female patients with acanthosis nigricans, ovarian hyperandrogenism and virilization [20]. Over 30 mutations have so far been described in these patients, which are mainly clustered in the tyrosine kinase domain of the insulin receptor [21, 22].

A nonsense mutation was identified in one allele of a patient substituting the termination codon (TGA) for the CGA codon normally encoding Arg^{331} located in a putative L2 domain, which is a single stranded right-hand beta-helix and is suggested to make up the bilobal ligand binding site [23]. The nonsense mutation at codon 331 truncated the C-terminal half of the receptor α subunit as well as the entire β subunit including the transmembrane anchor and the tyrosine kinase domain. Therefore, it is unlikely that this truncated receptor, translated from the mutant allele, would be either functional or located on the cell surface. In fact, extreme insulin resistance was observed in a female leprechaunism patient with homozygous R331X alleles.

Hyperinsulinemia is usually considered to be the result of resistance to the physiological effects of insulin and consequent compensatory increased insulin secretion. Recently, the C-peptide/insulin ratio is widely used as a surrogate of hepatic insulin clearance for the evaluation in type 2 DM or glucose intolerance [24, 25]. This index, should clarify whether impaired hepatic insulin clearance or increased insu-

lin secretion has a dominant effect on such patients. Insulin and C-peptide are secreted into the portal vein in a 1:1 molar ratio after β-cell stimulation by carbohydrate or other secretagogues. A large fraction of endogenous insulin is cleared by the liver, whereas C-peptide, which is cleared primarily by the kidney and has a lower metabolic clearance rate than insulin, and traverses the liver with essentially no extraction by hepatocytes [26, 27]. Diminished insulin clearance has been demonstrated to be an important underlying mechanism for the hyperinsulinemia found in various insulin-resistant conditions [28-30]. For example, to evaluate hyperinsulinemia in African Americans, at risk for type 2 DM, several studies used C-peptide/insulin molar ratio as an index of hepatic insulin clearance. African American children and adults showed lower C-peptide/insulin ratio than White Americans, thus suggesting that high insulin levels could be partly attributed to lower clearance [31, 32].

Therefore, the use of the C-peptide/insulin molar ratio reflects of hepatic insulin clearance [33]. A low C-peptide/insulin molar ratio of our patients suggests impaired hepatic insulin clearance because of, not only DM, but also abnormal insulin receptor expression in the liver. To this day, a low C-peptide/insulin molar ratio has not been substantially observed among individuals with type A insulin resistance. Two family cases with an insulin receptor gene mutation reported the presence of a low C-peptide/insulin molar ratio [34, 35]. They showed hyperinsulinemic hypoglycemia, severe insulin resistance and the C-peptide/insulin molar ratio ranged from 1.1 to 3.8.

As well as this reported cases, the molar ratio of the proband of our family was very low similar to that observed in subjects with insulin gene mutation. Previously, low C-peptide/insulin ratio was well reported to be a clinical feature of mutations in the human insulin gene causing either familial hyperinsulinemia or familial hyperproinsulinemia. The elevated circulating IRI consisted mainly of the unprocessed mutated proinsulin, which had accumulated because of proinsulin's relatively low clearance compared with insulin. In these subjects, proinsulin levels were tends to be extremely high, namely over three hundred pmol/L [36, 37]. Due to dramatic improvements in the assay techniques of IRI, cross-reactivity with proinsulin is normally seen at very low levels. Consequently, there have been no new reports regarding hyperproinsulinemia with insulin gene mutations for the last decade.

Recently, the fasting proinsulin/insulin ratio is used as a marker of β-cell dysfunction. In peripheral blood, fasting proinsulin accounts for 10-20% of insulin but it may reach values as high as 50 % in type 2 DM. Taura *et al.* evaluated the basal and dynamic proinsulin-insulin relationship to assess the β-cell function during OGTT in type 2 DM [38]. The proinsulin/insulin molar ratio was higher in type 2 DM (0.39 ± 0.05) subjects than normal (0.14 ± 0.01) and impaired glucose-tolerant (0.13 ± 0.02) subjects. In comparison to this study, the fasting proinsulin/insulin ratio of the proband, 0.20 was slightly higher than normal. It is difficult to consider that her low C-peptide/insulin molar ratio is derived from structural abnormalities in the proinsulin molecule.

We calculated the C-peptide/insulin molar ratio of several previous cases with insulin receptor gene mutation from data measured simultaneously. Severe cases, Rabson-Mendenhall syndrome or Donohue's syndrome, showed very low level (0.69 to 1.83) [14, 39-41]. Milder cases, type A insulin resistance or DM, also showed relatively low molar ratio (1.47 to 4.26) [35, 42]. However, most previous case reports only recorded the IRI data, more investigations are needed to discuss these clinical characteristics.

Interestingly, the patient's father did not show hyperinsulinemia while demonstrating a normal C-peptide/insulin molar ratio after fasting. However, after oral glucose ingestion, the insulin level increased 100.5 μU/mL/mL at 60 min and the molar ratio gradually decreased from 5.60 to 3.40. Meier *et al.* studied the C-peptide/insulin molar ratio as calculated at singular time points after oral glucose administration in non-diabetic subjects [37]. They reported that the molar ratio decreased to half level at 30 minutes and then it gradually increased up to the initial level through 120 min. In contrast to their data, the proband and her father showed a gradually decreasing pattern from 0 to 120 minutes. Receptor-mediated insulin endocytosis and degradation in hepatocyte underlie the basic mechanism of insulin clearance. Insulin is targeted for degradation after internalization, whereas the receptor recycles back to the cell surface [43]. CEACAM1, a transmembrane glycoprotein, plays a significant role in receptor-mediated insulin endocytosis [44]. *In vitro* studies suggest that upon its phosphorylation by the insulin receptor kinase, CEACAM1 binds indirectly to the receptor to undergo internalization in clathrin-coated vesicles as part of endocytosis complex [45].

CEACAM1 is considered to interact with two separate domains of the insulin receptor: a C-terminal for its phosphorylation, and cytoplasmic juxtamembrane domain required for internalization [46]. R331X mutant defects these important domains for endocytosis of insulin-insulin receptor complex. A reduction of endocytosis may also affect recycle of insulin receptor and may cause prolonged low hepatic extraction after glucose oral load observed in subjects having R331X mutation. Although her father showed normal data in fasting period, the oral glucose test may be a supplementary means for evaluating of insulin receptor mutant subjects.

As stated above, C-peptide is believed to be a better index of the pancreatic β-cell function than insulin because C-peptide levels are unaffected by hepatic clearance. When comparing the father's C-peptide levels of OGTT with proband, only a slight difference was observed. This result indicates that the insulin secreting function of β-cell is not substantially different and the cause of hyperinsulinemia in the proband is dominantly affected by impaired hepatic insulin clearance. The evaluation of the C-peptide/insulin molar ratio is thus considered to be a useful index for identifying genetic insulin resistance patients. On the other hand, a mild phenotype such as that observed in her father may not be effectively evaluated by the fasting data alone.

Unrelated Japanese patients with another mutation of the insulin receptor gene have been previously reported. They showed different phenotypes: one was detected as a heterozygous mutation in type A insulin resistance, while the other was detected as a compound heterozygous mutation in leprechaunism, thus indicating that the severity of such mutations will determine the phenotype [47]. The phenotype of heterozygous R331X differed substantially among the current family members. Although the proband and her grandmother showed diabetes mellitus with insulin resistance, the difference in the age of onset was around forty years. In addition, her father did not show insulin resistance after fasting. The reason for this difference may be conditioned by heredity and environment. The lifestyle for children has changed over the last few decades in Japan. The proband often consumed high caloric foods before detecting glucosuria. Numerous genetic factors related to diabetes mellitus have also been investigated. The insulin receptor pathway plays an important role in the glucose metabolism. The phenotype of a homozygous mutation, leprechaunism, revealed this important function in humans. However, a heterozygous mutation including Type A insulin resistance shows a mild phenotype. Variance in the current family case suggests that various genetic factors may therefore have played a role in their glucose metabolism. Contrary to expectations, the hypothesis that R331X determines the phenotype for glucose tolerance in Japanese people was ruled out. In addition, the influence of other reported mutations was unclear.

In conclusion, a nonsense mutation causing premature termination after amino acid 331 in the α subunit of the insulin receptor was identified in Japanese diabetes patients. The phenotype of R331X showed variety, and therefore further investigations, including determination of the mRNA level as well as ligand binding and receptor autophosphorylation, are thus called for to address the molecular mechanism by which this mutation leads to the occurrence of diabetes, as was observed in the current patient. In addition, the C-peptide/insulin molar ratio is considered to be a useful index for identifying genetic insulin resistance patients.

Acknowledgement

The study was supported in part by the Grants-in-Aid from the Japanese Ministry of Education, Culture, Sports, Science and Technology and the Global Center of Excellence (COE) program of Japan.

References

1. Massague J, Pilch PE, Czech MP (1980) Electrophoretic resolution of three major insulin receptor structures with unique subunit stoichiometries. *Proc Natl Acad Sci USA* 77: 7137-7141.
2. Kasuga M, Hedo JA, Yamada KM, Kahn CR (1982) The structure of insulin receptor and its subunits. Evidence for multiple nonreduced forms and a 210,000 possible proreceptor. *J Biol Chem 257*: 10392-10399.
3. Christiansen K, Tranum-Jensen J, Carlsen J, Vinten J (1991) A model for quaternary structure of human pla-

cental insulin receptor deduced from electron microscopy. *Proc Natl Acad Sci USA* 88: 249-252.
4. Ullrich A, Bell JR, Chen EY, Herrera R, Petruzzelli LM, TDull TJ, Gray A, Coussens L, Liao YC, Tsubokawa M, *et al.* (1985) Human insulin receptor and its relationship to tyrosine kinase family of oncogenes. *Nature* 313: 756-761.
5. Ebina Y, Ellis L, Jarnagin K, Edery M, Graf L, Clauser E, Ou JH, Masiarz F, Kan YW, Goldfine ID, *et al.* (1985) The human insulin receptor cDNA: the structural basis for hormone-activated transmembrane signaling. *Cell* 40: 747-758.
6. Kasuga M, Fujita-Yamaguchi Y, Blithe DL, Kahn CR (1983) Tyrosine-specific protein kinase activity is associated with the purified insulin receptor. *Proc Natl Acad Sci USA* 80: 2137-2141.
7. Rosen OM (1987) After insulin binds. *Science* 237: 1452-1458.
8. Taylor SI, Kadowaki T, Kadowaki H, Accili D, Cama A, McKeon C (1990) Mutations in insulin receptor gene in insulin-resistant patients. *Diabetes Care* 13: 257-279.
9. Taylor SI, Cama A, Accili D, Barbetti F, Quon MJ, de la Luz Sierra M, Suzuki Y, Koller E, Levy-Toledano R, Wertheimer E, *et al.* (1992) Mutation in the insulin receptor gene. *Endocri Rev* 13: 565-595.
10. Taylor SI (1992) Lessons from patients with mutation in the insulin-receptor gene. *Diabetes* 41: 1473-1490.
11. Taira M, Taira M, Hashimoto N, Shimada F, Suzuki Y, Kanatsuka A, Nakamura F, Ebina Y, Tatibana M, Makino H, *et al.* (1989) Human diabetes associated with a deletion of the tyrosine kinase domain of the insulin receptor. *Science* 245: 63-66.
12. Taylor SI, Accili D, Cama A, Kadowaki H, Kadowaki T, Imano E, Sierra ML (1991) Mutations in the insulin receptor gene in patients with genetic syndromes of insulin resistance. *Adv Exp Med Biol* 293: 197-213.
13. Longo N, Langley SD, Griffin LD, Elsas LJ (1992) Reduced mRNA and a nonsense mutation in the insulin receptor gene produce heritable severe insulin resistance. *Am J Hum Genet* 50: 998-1007.
14. Longo N, Wang Y, Smith SA, Langley SD, DiMeglio LA, Giannella-Neto D (2002) Genotype-phenotype correlation in inherited severe insulin resistance. *Hum Mol Genet* 11: 1465-1475.
15. Longo N, Singh R, Griffin LD, Langley SD, Parks JS, Elsas LJ (1994) Impaired growth in Rabson-Mendenhall syndrome: Lack of effect of growth hormone and insulin-like growth factor I. *J Clin Endocrinol Metab* 79: 799-805.
16. Kahn CR, Flier JS, Bar RS, Archer JA, Gorden P, Martin MM, Roth J (1976) The syndromes of insulin resistance and acanthosis nigricans. Insulin-receptor disorders in man. *N Eng J Med* 294: 739-745.
17. Bell GI, Picter RL, Rutter WJ, Cordell B, Tischer E, Goodman HM (1980) Sequence of the human insulin gene. *Nature* 284: 26-32.
18. Barbetti F, Gejiman PV, Taylor SI, Raben N, Cama A, Bonora E, Pizzo P, Moghetti P, Muggeo M, Roth J (1992) Detection of mutations in insulin receptor gene by denaturing gradient gel electrophoresis. *Diabetes* 41: 408-415.
19. Shier P, Watt VM (1983) Primary structure of a putative receptor for a ligand of the insulin family. *J Biol Chem* 264: 359-399.
20. Tritos NA, Mantzoros CS (1998) Syndromes of severe insulin resistance. *J Clin Endocr Metab* 83: 3025-3030.
21. Kadowaki H, Kadowaki T, Cama A, Marcus-Samuel B, Rovira A, Bevins CL, Taylor SI (1990) Mutagenesis of Lysine 460 in the human insulin receptor. *J Biol Chem* 265: 21285-21296.
22. Moller DE, Yokota A, White MF, Pazianos AG, Flier JS (1990) A naturally occurring mutation of insulin receptor alanine 1134 impaires tyrosine kinase function and is associated with dominantly inherited insulin resistance. *J Biol Chem* 265: 14979-14985.
23. Garrett TPJ, McKern NM, Lou M, Frenkel MJ, Bentley JD, Lovrecz GO, Elleman TC, Cosgrove LJ, Ward CW (1998) Crystal structure of the first three domains of the type-1 insulin-like growth factor receptor. *Nature* 394: 395-399.
24. Meier JJ, Holst JJ, Schmid WE, Nauck MA (2007) Reduction of hepatic insulin clearance after oral glucose ingestion is not mediated by glucagon-like peptide 1 or gastric inhibitory polypeptide in humans. *Am J Physiol Endocrinol Metab* 293: E846-E856.
25. Osei K, Rhinesmith S, Gaillard T, Schuster D (2003) Metabolic effects of chronic glipizide gastrointestinal therapeutic system on serum glucose, insulin secretion, insulin sensitivity, and hepatic insulin extraction in glucose-tolerant, first degree relatives of African American patients with type 2 diabetes: new insights on mechanisms of action. *Metabolism* 52: 565-572.
26. Horwitz DL, Starr JI, Mako ME, Blackard WG, Rubenstein AH (1975) Proinsulin, insulin, and C-peptide concentrations in human portal and peripheral blood. *J Clin Invest* 55: 1278-1283.
27. Shapiro ET, Tillil H, Miller MA, Frank BH, Galloway JA, Rubenstein AH, Polonsky KS (1987) Insulin secretion and clearance. Comparison after oral and intravenous glucose. *Diabetes* 36: 1365-1371.
28. Polonsky KS, Given BD, Hirsch L, Shapiro ET, Tillil H, Beebe C, Galloway JA, Frank BH, Karrison T, Van Ceuter E (1988) Quantitative study of insulin secretion and clearance in normal and obese subjects. *J Clin Invest* 81: 435-441.
29. Jones CNO, Pei D, Staris P, Polonsky KS, Ida Chen YD, Reaven GM (1997) Alternations in the glucose-stimulated insulin secretory dose-response curve and in insulin clearance in nondiabetic insulin-resistant indi-

viduals. *J Clin Endocrinol Metab* 82: 1834-1838.
30. Inokuchi T, Watanabe K, Kameyama H, Orita M (1988) Altered basal C-peptide/insulin molar ratio in obese patients with fatty liver. *Jpn J Med* 27: 272-276.
31. Arslanian SA, Saad R, Lewy V, Danadian K, Janosky J (2002) Hyperinsulinemia in African-American Children. *Diabetes* 51: 3014-3019.
32. Osei K, Schster DP, Owusu SK, Amoah AG (1996) Race and ethnicity determine serum insulin and C-peptide concentrations and hepatic insulin extraction and insulin clearance: comparative studies of three populations of West African ancestry and white Americans. *Metabolism* 46: 53-58.
33. Polonsky KS, Rubenstein AH (1984) C-peptide as a measure of the secretion and hepatic extraction of the insulin. Pitfalls and limitations. *Diabetes* 33: 486-494.
34. Højlund K, Hansen T, Lajer M, Henriksen JE, Levin K, Lindholm J, Pedersen O, Beck-Nielsen H (2004) A novel syndrome of autosomal-dominant hyperinsulinemic hypoglycemia linked to a mutation in the human insulin receptor gene. *Diabetes* 53: 1592-1598.
35. Huang Z, Li Y, Tang T, Xu W, Liao Z, Yao B, Hu G, Weng J (2009) Hyperinsulinaemic hypoglycemia associated with a heterozygous missense mutation of R1174W in the insulin receptor (IR) gene. *Clin Endocrinol* 71: 659-665.
36. Røder ME, Vissing H, Nauck MA (1996) Hyperproinsulinemia in a three-generation Caucasian family due to mutant proinsulin (Arg65→His) not associated with impaired glucose tolerance: the contribution of mutant proinsulin to insulin bioactivity. *J Clin Endocrinol Metab* 81: 1634-1640.
37. Meier JJ, Gallwitz B, Siepmann N, Holst JJ, Deacon CF, Schmidt WE, Nauck MA (2003) The reduction in hepatic insulin clearance after oral glucose is not mediated by gastoric inhibitory polypeptide (GIP). *Regul Pept* 113: 95-100.
38. Taura A, Pacini G, Kautzky-Willer A, Ludvik B, Prager R, Thomaseth K (2003) Basal and dynamic proinsulin-insulin relationship to assess β-cell function during OGTT in metabolic disorders. *Am J Physiol Endocrinol Metab* 285: E155-E162.
39. Thiel CT, Knebel B, Knerr I, Sticht H, Müller-Wieland D, Zenker M, Reis Andre, Dörr HG, Rauch A (2008) Two novel mutations in the insulin binding impairment in a patient with Rabson-Mendenhall syndrome. *Mol Genet and Metab* 94: 356-362.
40. Unal S, Aycan Z, Halsall DJ, Kibar AE, Eker S, Ozaydin E (2009) Donohue syndrome in a neonate with homozygous deletion of exon 3 of the insulin receptor gene. *J Pediatr Endocrinol Metab* 22: 669-674.
41. Tuthill A, Semple RK, Day R, Soos MA, Sweeney E, Seymour PJ, Didi M, O'Ragilly S (2007) Functional characterization of a novel insulin receptor mutation contributing to Rabson-Mendenhall syndrome. *Clin Endocrinology* 66: 21-26.
42. Riqué S, Nogués C, Ibáñez L, Marcos MV, Ferragut J, Carrascosa A, Potau N (2000) Identification of three novel mutations in the insulin receptor gene in type A insulin resistant patients. *Clin Genet* 57: 67-69.
43. Carpentier JL (1993) Robert Feulgen Prize Lecture 1993. The journey of the insulin receptor into the cell: from cellular biology to pathophysiology. *Histochemistry* 100: 169-184.
44. Poy MN, Yang Y, Rezaei K, Fernström MA, Lee AD, Kido Y, Erickson SK, Najjar SM (2002) *Nature Genet* 30: 270-276.
45. Choice CV, Howard MJ, Poy MN, Hankin MH, Najjar SM (1998) *J Biol Chem* 273: 22194-22200.
46. Najjar SN (2002) Regulation of insulin action by CEACAM1. *Trends Endocrinol Metab* 13: 240-245.
47. Kadowaki H, Takahashi Y, Ando A, Momomura K, Kaburagi Y, Quin JD, MacCuish AC, Koda N, Fukushima Y, Taylor SI, Akanuma Y, Yazaki Y, Kadowaki T (1997) Four mutant alleles of the insulin receptor gene associated with genetic syndromes of extreme insulin resistance. *Biochem. Biophys. Res. Commun* 237: 516-520.

Genetic Variants in Pigment Epithelium-Derived Factor Influence Response of Polypoidal Choroidal Vasculopathy to Photodynamic Therapy

Isao Nakata, MD,[1,2] Kenji Yamashiro, MD, PhD,[1] Ryo Yamada, MD, PhD,[2] Norimoto Gotoh, MD,[1,2] Hideo Nakanishi, MD, PhD,[1,2] Hisako Hayashi, MD,[1,2] Akitaka Tsujikawa, MD, PhD,[1] Atsushi Otani, MD, PhD,[1] Sotaro Ooto, MD, PhD,[1] Hiroshi Tamura, MD, PhD,[1] Masaaki Saito, MD, PhD,[3] Kuniharu Saito, MD,[3] Tomohiro Iida, MD, PhD,[3] Akio Oishi, MD, PhD,[4] Yasuo Kurimoto, MD, PhD,[4] Fumihiko Matsuda, PhD,[2] Nagahisa Yoshimura, MD, PhD[1]

Purpose: To investigate whether photodynamic therapy (PDT) outcomes of polypoidal choroidal vasculopathy (PCV) are related to baseline clinical characteristics, smoking history, or genetic factors by analyzing the retreatment-free period after the first PDT.

Design: Retrospective cohort study.

Participants: The study consisted of 167 patients with PCV who underwent PDT as their first treatment.

Methods: We targeted 638 single nucleotide polymorphisms (SNPs) in 42 possible susceptible genes for age-related macular degeneration to evaluate their relation to the effectiveness of PDT for PCV. For this evaluation, we used 2 methods: (1) survival analysis, with the retreatment-free period as the target; and (2) logistic regression test between the need for additional therapy within 3 months after the first PDT and the genotypes, with age, gender, smoking status, and greatest linear dimension (GLD) at baseline as covariates. The contributions of smoking status and GLD at baseline for the retreatment-free period also were evaluated. Contributions of these factors to visual prognosis were evaluated for 1 year after PDT.

Main Outcome Measures: Retreatment-free period after the first PDT for PCV. Secondary outcome measures included correlation of the susceptible factor to the retreatment requirement within the 3-month follow-up and the mean visual acuity change.

Results: In survival analyses, SERPINF1 rs12603825 showed a significant association with the retreatment-free period after the first PDT; those patients homozygous for the minor allele A of rs12603825 received additional treatment after PDT within significantly shorter times than those with other genotypes ($P = 0.0038$). There was no significant difference in the retreatment-free period between baseline GLD and smoking status. Retreatment within 3 months was required significantly more in patients with the AA genotype, even after taking into consideration the effect of clinical characteristics (age, gender), baseline PCV lesion size, and smoking status ($P = 0.0027$). Furthermore, patients with the AA genotype showed significantly worse visual prognosis after PDT ($P = 0.013$).

Conclusions: Pigment epithelium-derived factor (SERPINF1 or PEDF) polymorphisms may influence the initial response to and visual prognosis after PDT for PCV. Our findings may lead to understanding the pathogenesis of PCV and modification of the effects of PDT.

Financial Disclosure(s): The author(s) have no proprietary or commercial interest in any materials discussed in this article. *Ophthalmology 2011;xx:xxx © 2011 by the American Academy of Ophthalmology.*

Polypoidal choroidal vasculopathy (PCV) is observed frequently in Asian patients diagnosed with exudative age-related macular degeneration (AMD),[1,2] and PCV recently has been considered to be a separate clinical entity differing from neovascular AMD and other diseases associated with subretinal neovascularization.[3] Recent studies on the genetics of AMD and PCV have recognized them as complex diseases caused by the actions and interactions of numerous genes and environmental factors.[4–8]

Photodynamic therapy (PDT) with verteporfin was previously one of the main therapeutic options for neovascular AMD, and several studies have shown that the treatment effects of PDT for AMD vary according to the baseline composition, including lesion size of choroidal neovascularization, visual acuity, and genotype.[9–12] Many studies have reported that PDT is more effective in treating PCV than neovascular AMD,[13–15] although PDT for PCV often has to be repeated, either because of persistent disease or

ISSN 0161-6420/11/$–see front matter
doi:10.1016/j.ophtha.2010.12.011

recurrence.[16,17] There are limited reports of the association between clinical or pathologic features and the response of PCV to PDT. When evaluating the effect of PDT for PCV, it is essential to consider both genetic and environmental factors, which has been done in the evaluation of AMD. As shown in the AMD study, studies have shown that smoking is associated with the development of PCV.[18–20]

The objectives of the current study were to discern whether the response of PCV to PDT was related to baseline clinical characteristics, smoking history, and genetic background by analyzing multiple single nucleotide polymorphisms (SNPs) and focusing primarily on the clinical retreatment-free period.

Materials and Methods

All procedures in this study adhered to the tenets of the Declaration of Helsinki. The institutional review board and ethics committee of each institute involved approved the protocols of this study. All patients were fully informed of the purpose and procedures of this study, and written consent was obtained from each patient.

Patients and Methods

The study consisted of 167 Japanese patients with PCV who underwent PDT at Kyoto University Hospital, Fukushima Medical University Hospital, or Kobe City Medical Center General Hospital between August 2004 and February 2009. All patients enrolled in the study met the criteria of PCV as proposed by the Japanese Study Group of Polypoidal Choroidal Vasculopathy.[21] Each subject underwent a complete ophthalmic examination, including measurement of best-corrected visual acuity, indirect ophthalmoscopy and slit-lamp biomicroscopy with a contact lens by a retina specialist, fluorescein angiography and indocyanine green angiography (ICGA), and optical coherence tomography. Best-corrected visual acuity was measured with a Landolt chart and converted to a logarithm of the minimal angle of resolution for statistical analysis. The inclusion criteria for this study were (1) diagnosis of PCV, (2) treatment with PDT as the first therapy, (3) age $\geq$ 50 years, (4) presence of a subfoveal lesion, and (5) best-corrected Snellen visual acuity equivalent of 20/200 to 20/40 at baseline. Exclusion criteria were (1) choroidal neovascularization caused by other diseases (e.g., pathologic myopia, uveitis) and (2) combined treatment (e.g., PDT in combination with antivascular endothelial growth factor drugs). If a patient had bilateral PCV treated with PDT, the eye treated earlier that fulfilled the criteria of this study was selected as the study eye for analysis. The greatest linear dimension (GLD) used for PDT was based on the ICGA findings and covered the entire PCV vascular lesion, including polypoidal lesions and branching vascular network vessels.[22] All patients received PDT with verteporfin following the standard protocol of treatment[23] except for determination of the GLD. At 3 months after the first PDT for PCV, all patients underwent a repeat ophthalmologic examination, including optical coherence tomography or fluorescein angiography and ICGA, on which the need for additional treatment was based. This sequence was followed during the follow-up time at intervals of patient visits to the outpatient clinic for up to 3 months. The retreatment-free period was calculated as the date of the first PDT to the date that the treating physician opted for additional treatment for a persistent or new lesion.

To evaluate the effect of GLD size, patients were divided into 3 groups according to the guidelines for PDT in Japan.[24] The GLD was $\leq$1800 μm in the first group, 1800 to 5400 μm in the second group, and $\geq$5400 μm in the third group. Information on smoking status (never smoked, ex-smoker, or current smoker) was obtained by self-reported questionnaire.

Two methods were used for the current PDT study: (1) survival analysis, with the retreatment-free period after the first PDT being the target; and (2) logistic regression test between 2 subgroups to evaluate the initial response to PDT. Because additional treatment with PDT is usually considered at 3 months after the first PDT,[14,25] the patients were classified into 1 of 2 groups by whether additional treatment was required within the first 3-month follow-up. Those patients who required additional therapy within 3 months after the first PDT (i.e., they continued to show an exudative lesion or had a worsened exudative lesion) were regarded as having a retreatment-free period of less than 3 months (Fig 1).

Multiplexing Single Nucleotide Polymorphism Analysis

To identify susceptible SNPs for the retreatment-free period after the first PDT, we used 31 of 160 PCV samples that were genotyped with the Illumina GoldenGate assay across 638 SNPs of 42 genes on a BeadStation 500G Genotyping System (Illumina, Inc., San Diego, CA); this was customized to evaluate possible AMD/PCV susceptible genes (listed in Table 1, available at http://aaojournal.org.). Haploview[26] software was used to infer the linkage disequilibrium (LD) in the targeted regions; among the candidate SNPs, LD indices (D' and r^2) were calculated with Haploview. To detect an association between the gene and the response to PDT, 1 representative SNP was chosen from each region. To confirm the positive association seen in the screening samples, 136 additional patients were genotyped for the SNPs with the Taqman SNP assay, which used the ABI PRISM 7700 system (Applied Biosystems, Foster City, CA). The 31 PCV samples used in the initial screening were also genotyped to validate concordance between the GoldenGate assay and the Taqman assay. Samples with a low successful call rate (<95%) were excluded from the study.

Statistical Analyses

Survival analysis was conducted using Kaplan–Meier methods to estimate differences among genotypes in the retreatment-free period after the first PDT. The retreatment-free period of the patients with no additional treatment was censored at the time of last contact. To detect differences in survival, Breslow–Gehan–Wilcoxon tests were used. When a significant association was found, the best fitting model (additive, dominant, or recessive) was then investigated. The Hardy–Weinberg equilibrium for genotypic distribution was evaluated using the Hardy–Weinberg equilibrium exact test. Descriptive statistics for all demographic and clinical variables were calculated and comparisons were made using the unpaired *t* test for means with continuous data (e.g., age) and the chi-square test for categoric data (e.g., gender). Logistic regression analysis was used to evaluate the association for adjusting age, gender, smoking status, GLD, and genotype considering the best fitting model. Visual prognosis after treatment was compared by a repeated-measures analysis of variance. *P* value correction was performed with the Bonferroni method using the ratio of the number of all genotyped SNPs in the screening procedure. For overall survival analysis, *P* value correction was performed with the Bonferroni method using the ratio of the number of

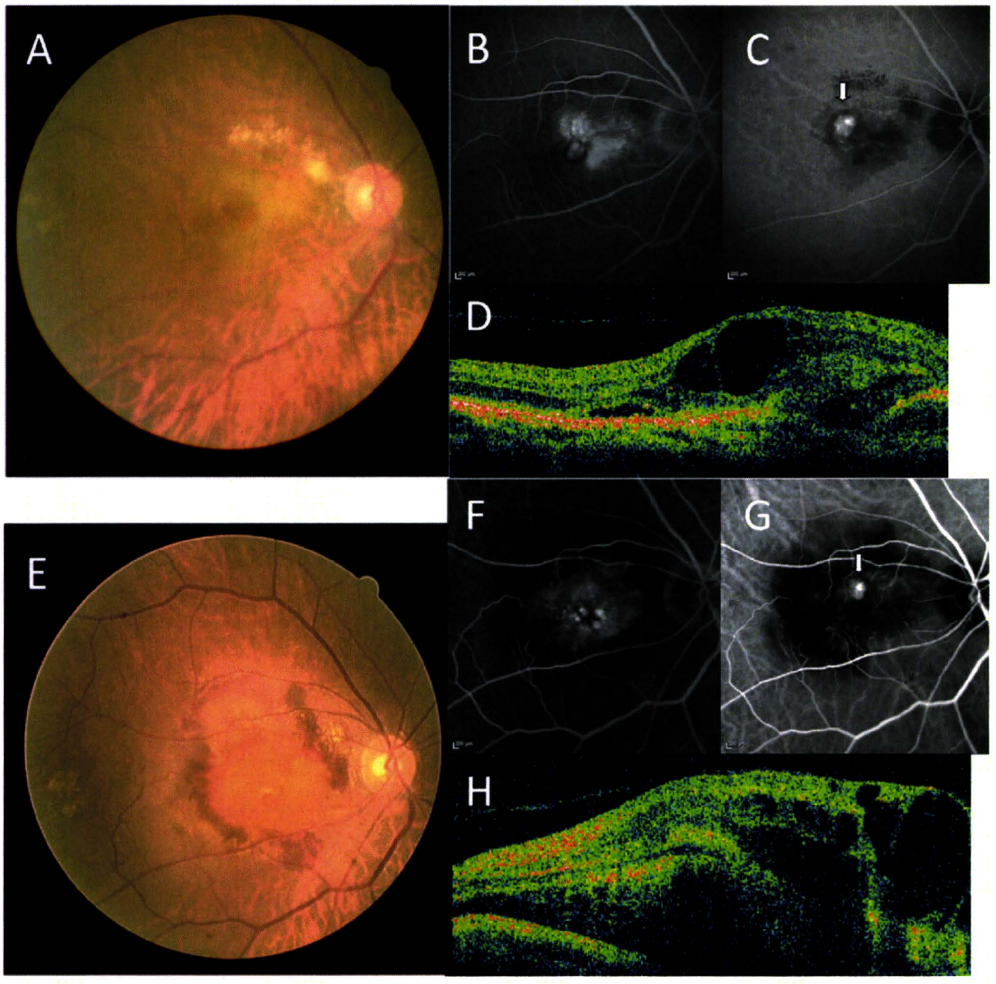

Figure 1. Fundus photographs **(A, E)**, fluorescein angiographs **(B, F)**, indocyanine green angiographs **(C, G)**, and optical coherence tomographs **(D, H)** of a patient who received additional treatment within 3 months after the first PDT. This 72-year-old man with PCV in his right eye underwent PDT as his first therapy. Before the treatment **(A–D)**, his best-corrected visual acuity was 20/200 and ICGA revealed an active polyp **(C,** *white arrow*). Seventy-six days after PDT **(E–H)**, the treating physician opted to perform additional treatment because his best-corrected visual acuity decreased to 20/400, a new macular hemorrhage appeared, and the polyp **(G,** *white arrow*) and exudative lesion **(F, H)** remained active.

selected SNPs from the screening. Significance was defined at the 5% level.

Results

A total of 167 patients with PCV who underwent PDT as their first therapy at 1 of 3 institutes were enrolled in the current study. Demographic and clinical characteristics of each patient by institute involved are shown in Table 2.

Survival Analysis for the Retreatment-free Period

Of the 160 patients with PCV who were genotyped by the Illumina GoldenGate assay, which launches 638 SNPs across 42 genes in our previous study, 31 met the inclusion criteria of the current PDT study and were used for the screening of genotype data. Because 57 SNPs with no call or scattered or overlapping clusters were excluded from the analysis, 581 SNPs were evaluated by survival analysis with the retreatment-free period. We identified 6 SNPs in 4 genes (FBLN5, CX3CR1, SERPINF1, and TLR4), with the P value adjusted for multiple testing <0.05 (Table 3). At SERPINF1 gene, rs12103559 and rs1894286 were in strong LD (pair-wise D' = 1.0 and r^2 = 1.0). By considering the LD and minor allele frequency of 3 SNPs of this region, we selected rs12603825 as the representative SNP of the SERPINF1 gene and tested a total of 4 SNPs in other patients. A total of 136 additional patients from the 3 institutes were genotyped by the Taqman method. Genotyping success rates of the 4 SNP markers in the additional 136 samples were greater than 98.8%. In overall survival analyses, SERPINF1 rs12603825 showed a significant association with the retreatment-free period (P = 0.0117). Patients homozygous for the minor allele of rs12603825 (i.e., a recessive model) were given an additional treatment after the first PDT in significantly shorter time periods than were the other genotypes (P = 0.0038), and this association remained significant after a permutation procedure for multiple test correction (corrected P = 0.015) (Table 3, Fig 2).

There was no significant difference in the retreatment-free period among the 3 GLD groups and the smoking status groups